LAWRENCE
LIVERMORE
NATIONAL
LABORATORY

LLNL-TR-813880

Heat Loss Correction Factor for Fireball Yield Measurements

Anna V. Costelle
Arizona State University

HEDP Summer Student
WCI-DP

Mentor: G. D. Spriggs and Andy Cook

August 14, 2020

Auspices Statement

This work was performed under the auspices of the U.S. Department of Energy by Lawrence Livermore National Laboratory under Contract DE-AC52-07NA27344

Heat Loss Correction Factor for Fireball Yield Measurements

A.V. Costelle

Lawrence Livermore National Laboratory

Livermore, California

Introduction

Fireball yield calculations are performed using Taylor's radius equation,

$$R = R_0(\frac{\theta Y_{sw}}{\rho_a})^{1/5} t^{2/5} \quad (1)$$

where R is the radius (m) of the shock wave, R_0 is a proportionality constant that depends on γ, Y_{sw} is the energy (kt) of the shock wave, θ is the geometric factor, ρ_a is the air density ($\mathrm{kg/m^3}$) at the height of burst, and *t* is time (s). Then, we can say that

$$R_1 = R_0(\frac{\theta Y_{sw}}{\rho_a})^{1/5} \quad (2)$$

and rewrite (1), such that

$$R = R_1 t^{2/5} \quad (3)$$

Then, in addition to (2), R_1 can also be written in the following form

$$R_1 = \frac{R}{t^{2/5}} \quad (4)$$

However, at early times, the x-ray diffusion process has a significant effect on the size of the fireball, and at late times the shock wave degenerates into an acoustic wave. Thus, earlier research determined that the range of validity for Taylor's equation was in the scaled time regime of 0.004–0.008 s. So, when performing a yield calculation, the only values of (4) that are analyzed are those that lie within that range of validity, where scaled time can be defined as

$$t_{scaled} = t(\frac{\rho_a}{\theta Y})^{1/3} \quad (5)$$

Within that scaled time regime, the value of R_1 is approximately constant. Then scaled yield can be determined from the equation,

$$\frac{\theta Y_{sw}}{\rho_a} = (\frac{R_1}{R_0})^5 \quad (6)$$

While Taylor's equations offer an approximation of the scaled yield, they also rely on several assumptions. For example, the equations assume that the shock wave is adiabatic, when, in fact, the first light pulse on the nuclear test films, which occurs as the shock wave is forming, suggests that the shock wave is not adiabatic. Furthermore, the amount of heat loss from the shock wave that occurs prior to the scaled time regime of 0.004–0.008 s can change significantly as a function of air density. This may cause the shock wave radius to be smaller relative to the assumed adiabatic shock wave. Therefore, the objective of this project was to determine the correction factor for heat transfer, which should be applied to (5) in order to produce a more accurate approximation of the weapon's yield.

Methodology

Using the state-of-the-art hydrodynamics code Miranda, a series of nuclear detonations were simulated at different air densities. Table 1 outlines the specific data for each case.

Table 1. Outline of the input data for the simulations run in Miranda

Case	Type	Yield (kt)	Rho ($\mathbf{kg/m^3}$)	Relative Humidity
1	Airdrop	1	1.22	0%
2	Airdrop	1	1.0	0%
3	Airdrop	1	0.8	0%
4	Airdrop	1	0.6	0%
5	Airdrop	1	0.6	100%
6	Airdrop	1	0.4	0%
7	Airdrop	1	0.2	0%
8	Airdrop	1	0.1	0%
9	Airdrop	1	0.05	0%

Note: Each case listed was composed of two simulations—one with heat transfer turned off and one with heat transfer turned on.

For each case, we ran two simulations in Miranda. First, heat transfer physics was turned off. Thus, the shock wave was adiabatic. A second simulation was run using the same input data for that case but with heat transfer physics turned on. The R_1 value was calculated for both the adiabatic and nonadiabatic run in each case as a function of time using (4). Then scaled time was calculated using (5). The final R_1 value for each simulation was determined by taking the average of the R_1 values within the scaled time regime 0.004–0.008 s, as the value should be relatively constant in that regime. The correction factor was then defined as

$$C = \left(\frac{R_{1ad}}{R_{1hl}}\right)^5 \qquad (7)$$

where R_{1ad} is the final R_1 value from the adiabatic simulation, and R_{1hl} is the final R_1 value from the nonadiabatic simulation.

Additionally, it should be noted that all cases were airdrops, meaning that the geometric factor, θ, was 1. Furthermore, the relative humidity in case 5 was set to 100% to determine whether humidity may also have an effect on the radius of the shock wave, which would indicate a need for further research into the combined effect of air density and humidity.

Results and Conclusions

After conducting the 18 simulations that composed the 9 cases outlined in Table 1, the results were amalgamated to find the correction factor for heat loss as a function of air density. The results are summarized in Table 2.

Table 2. Summary of calculations performed from simulations results

Rho ($\mathbf{kg/m^3}$)	Relative Humidity	R_1 (Adiabatic Simulation)	R_1 (Heat Transfer Simulation)	Correction Factor for Heat Loss
1.22	0%	278.43	278.58	0.9972
1.0	0%	279.47	279.54	0.9987
0.8	0%	280.57	280.50	1.0013
0.6	0%	281.66	281.69	0.9996
0.6	100%	280.58	280.45	1.0023
0.4	0%	283.52	283.41	1.0020
0.2	0%	286.40	286.49	0.9984
0.1	0%	289.21	289.60	0.9933
0.05	0%	291.80	292.44	0.9887

Note: The simulation provided shock wave radius and volume data as a function of time. Scaled time was calculated using (5) and R_1 values for both adiabatic and heat transfer simulations, shown in the table, were determined using (4) in the specified scaled time regime. The correction factor was then determined from (7).

The results summarized in Table 2 reveal that, at all air densities, there is very little difference between the radius of an adiabatic shock wave, and that of a shock wave with heat transfer. Thus, at all air densities, the correction factor was approximately 1.0. At an air density of 0.05 $\mathrm{kg/m^3}$, there is a slightly more profound difference between the adiabatic and nonadiabatic shock waves, but, even then, it is still minimal.

However, at an air density of 0.6 $\mathrm{kg/m^3}$, there was a notable difference between the R_1 values of the simulations with 0% humidity and those with 100% humidity. Thus, although heat transfer seemed to have little effect on the R_1 values, there was an effect due to humidity, which should be accounted for in yield calculations. In order to explore this effect further, another simulation was run at each of the other eight air densities, with humidity set to 100%. Again, the R_1 values for each of those simulations were calculated using (4), then scaled time was calculated using (5), and the average R_1 was found in the scaled time regime of 0.004–0.008 s. See the results of the simulations with 100% humidity and heat transfer turned on in Table 3.

Table 3. Summary of the calculations using data from the second round of simulations

Rho ($\mathbf{kg/m^3}$)	Relative Humidity	$\boldsymbol{R_1}$ (Heat Transfer on)
0.05	100%	290.98
0.1	100%	288.31
0.2	100%	285.16
0.4	100%	282.10
0.6	100%	280.45
0.8	100%	279.47
1.0	100%	278.37
1.22	100%	277.46

Note: Heat transfer physics was turned on for all runs and the relative humidity was set to 100%. Since heat transfer was shown to have little effect on the radius, this data set was intended to help in analyzing the effect of humidity.

Comparing the values in Table 2 and Table 3, the R_1 values in the cases with higher humidity are consistently lower than those of the cases with no humidity, confirming the assumption from the original data set that there was an effect due to humidity.

Another noteworthy result is that R_1 changed more drastically than expected, as a function of air density. From equation (2), with θ and Y both being held constant at 1, R_1 should decrease as air density increases, and have an instantaneous slope of $\frac{R_0}{5\rho_a^{6/5}}$ where R_0 is a constant.

However, when R_1 was plotted as a function of air density, the rate of change was slower than expected, as seen in Figure 1.

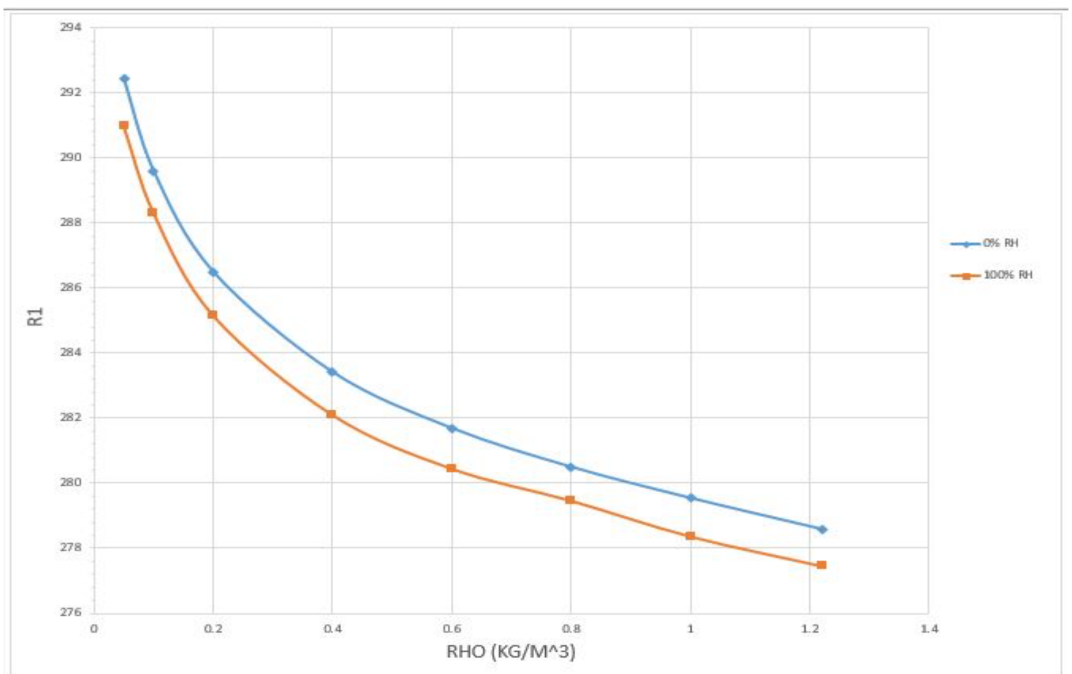

Figure 1. R_1 values from simulations with heat transfer plotted as a function of air density. The blue data is from simulations with 0% humidity and the orange data is from simulations with 100% humidity.

Because the R_1 data is not parallel to the expected slope, we can see from equation (2) that the assumption that R_0 is constant must be incorrect. So, R_0 must be changing as a function of air density. Since R_0 depends on γ of air, it must be that γ is changing with air density, which should be accounted for in yield calculations. In order to correct for this unexpected change, first, a relative correction factor was determined by dividing all R_1 values at both 0% and 100% humidity by the R_1 value at an air density of 1.0 $\mathrm{kg/m^3}$ and 0% humidity. Then, to find the general correction factor for γ, the inverse of the relative correction factor was raised to the fifth power, such that the corrected scaled yield can be expressed as

$$\frac{\theta Y}{\rho_a} = C(\frac{R_1}{R_0})^5 \tag{8}$$

where C is the correction factor for γ. Plotting the calculated correction factors as a function of air density in cases with both 0% and 100% humidity yields the graph in Figure 2.

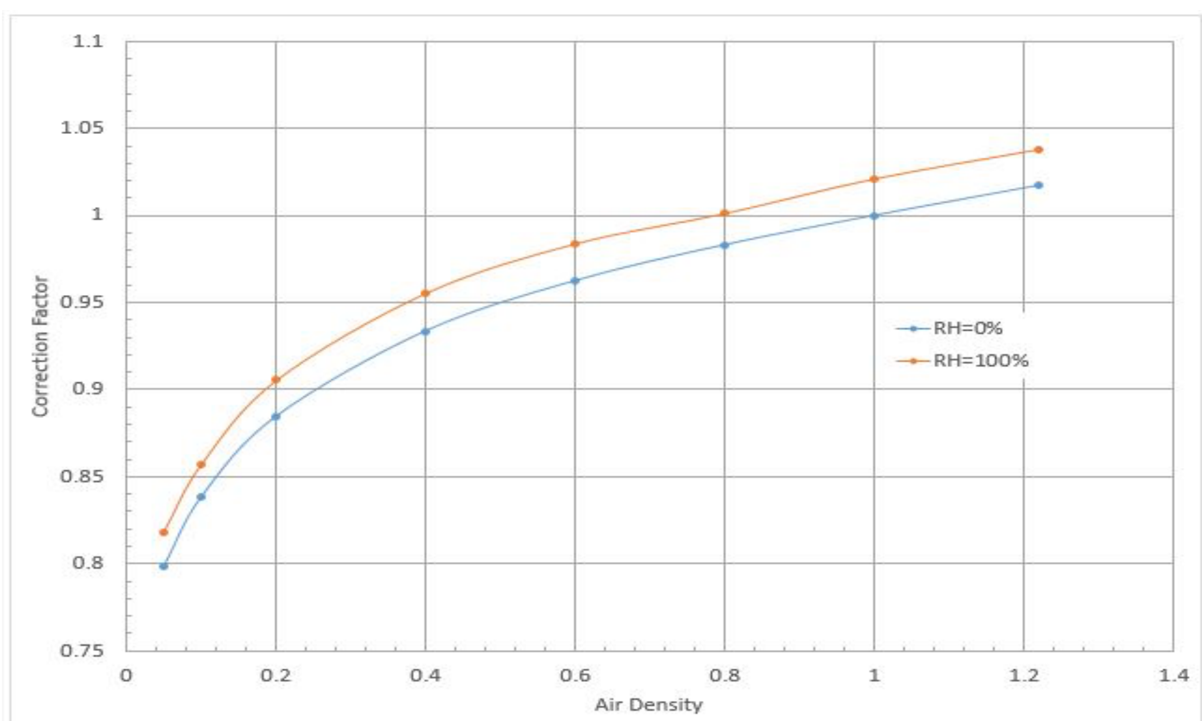

Figure 2. Plot of the γ correction factor as a function of air density. The blue data corresponds to 0% humidity and the orange data corresponds to 100% humidity.

The results of this project indicate that the correction for heat loss is approximately 1 at all air densities and any humidity. However, humidity in and of itself had an effect on R_1 and thus, on the yield calculation for the weapon in question. Furthermore, the data indicated that R_0 and therefore, γ are not constant. Rather, they change as a function of air density. Figure 2 illustrates the correction factor for these changes, at both 0% and 100% humidity, as a function of air density. Future work on this project should focus on finding the γ correction factor solution curves at other humidity percentages, in order to generate a more comprehensive understanding of the combined effect of humidity and changes in γ as a function of air density on the calculated yield of the weapon.

REFERENCES

J. D. RAMSHAW AND A. W. COOK, “APPROXIMATE EQUATIONS OF STATE IN TWO-TEMPERATURE PLASMA MIXTURES,” PHYSICS OF PLASMAS **21**, 022706 (2014). LLNL-JRNL-643493

A. W. COOK, “'EFFECTS OF HEAT CONDUCTION ON ARTIFICIAL VISCOSITY METHODS FOR SHOCK CAPTURING,” J. COMPUT. PHYS. **255**, 48–52 (2013). LLNL-JRNL-608332

A. W. COOK, "ENTHALPY DIFFUSION IN MULTICOMPONENT FLOWS," PHYS. FLUIDS **21**, 055109 (2009). LLNL REPORT NO. LLNL-JRNL-408798

A. W. COOK, "ARTIFICIAL FLUID PROPERTIES FOR LARGE-EDDY SIMULATION OF COMPRESSIBLE TURBULENT MIXING," PHYS. FLUIDS **19**, 055103 (2007). LLNL REPORT NO. UCRL-CONF-227155

A. W. COOK AND W. H. CABOT, "HYPERVISCOSITY FOR SHOCK-TURBULENCE INTERACTIONS," J. COMPUT. PHYS. **203**, 379-385 (2005). LLNL REPORT NO. UCRL-JRNL-202570

A. W. COOK AND W. H. CABOT, "A HIGH-WAVENUMBER VISCOSITY FOR HIGH-RESOLUTION NUMERICAL METHODS," J. COMPUT. PHYS. **195**, 594-601 (2004). LLNL REPORT NO. UCRL-ID-152002

A. W. COOK, "A CONSISTENT APPROACH TO LARGE EDDY SIMULATION USING ADAPTIVE MESH REFINEMENT," J. COMPUT. PHYS. **154**, 117-133 (1999). LLNL REPORT NO. UCRL-JC-132402

A. W. COOK AND J. J. RILEY, "SUBGRID-SCALE MODELING FOR TURBULENT REACTING FLOWS," COMBUST. FLAME **112**, 593-606 (1998).

A. W. COOK, J. J. RILEY, AND G. KOSALY, "A LAMINAR FLAMELET APPROACH TO SUBGRID-SCALE CHEMISTRY IN TURBULENT FLOWS," COMBUST. FLAME **109**, 332-341 (1997).

A. W. COOK AND J. J. RILEY, "DIRECT NUMERICAL SIMULATION OF A TURBULENT REACTIVE PLUME ON A PARALLEL COMPUTER," J. COMPUT. PHYS. **129**, 263-283 (1996).

A. W. COOK AND J. J. RILEY, "A SUBGRID MODEL FOR EQUILIBRIUM CHEMISTRY IN TURBULENT FLOWS," PHYS. FLUIDS **6**, 2868-2870 (1994).